Noise effects on gap wave propagation in a nonlinear discrete *LC* transmission line

Serge Bruno Yamgoué,* Savério Morfu,† and Patrick Marquié‡
Laboratoire d'Electronique, Informatique et Image, UMR CNRS 5158, Dijon, UFR Sciences et Techniques, Université de Bourgogne 9, allée Alain Savary, BP 47870, 21078 Dijon Cedex, France
(Received 25 September 2006; revised manuscript received 28 November 2006; published 16 March 2007)

We report here the results of numerical investigation of noise effects on the propagation in a nonlinear waveguide modeled by a discrete electrical line. Considering a periodic signal of frequency exceeding the natural cutoff frequency of this system, we show that noise can be used to trigger soliton generation in the medium. Besides the classical stochastic resonance signature exhibited by each oscillator of the network, our simulation results reveal in particular that the signal-to-noise ratio remains almost constant in the whole network for an appropriate amount of noise. This interesting feature insures for the generated solitons a quality preserved propagation along the network.

DOI: 10.1103/PhysRevE.75.036211 PACS number(s): 05.10.Gg, 05.40.Ca, 05.45.Yv, 05.45.Xt

I. INTRODUCTION

The counter-intuitive fact that noise may play a beneficial role in some nonlinear systems' dynamics was originally introduced in the context of geophysical dynamics [1–3]. Like the two other nonlinear features that are chaos and solitons, it has then been progressively reported in a broad variety of systems pertaining to different domains of science. Accordingly, a continuously growing attention is currently devoted to its investigation.

This phenomenon has been primarily studied in a model consisting of a heavily damped particle embedded in a symmetric double-well potential, and subjected to a sinusoidal driving [4]. When the amplitude of this force is weak (below a critical value depending on the potential barrier) the particle can only oscillate in the well in which its motion is started. It has been observed that, in this subthreshold situation, hopping of the particle from one well to the other can be triggered and synchronized in a statistical sense to this weak driving, by an optimal amount of noise [4]. This is readily referred to as stochastic resonance.

Several models of nonlinear systems, still of single degree of freedom, have subsequently been shown to exhibit stochastic resonance features, according to some performance measure which, usually, is the so-called signal-to-noise ratio (SNR). These include monostable smooth single-well potentials [5–8], excitable systems [9–11] and threshold devices [12,13]. One and two dimensional arrays of such stochastic resonators have also been considered, and the enhancement of stochastic resonance [14] and of propagation have been proven [8,15–18]. Stochastic resonance for biharmonic forcing has also been studied [19].

On the other hand, owing to the observation of solitons in a variety of natural phenomena, including crystal lattice vibrations [20], water and plasma waves [21,22], and energy transport in proteins [22], to name just a few, solitons bearing systems have attracted considerable attention from researchers for about half a century now. This interest is also motivated by the potential applicability of solitons. As an important example, soliton concepts have been used in optical telecommunications to achieve spectacular progresses in terms of transmission capacities [23,24].

Thus, the stochastic resonance features just defined above may undoubtedly be of great importance for information transmission in telecommunications. Indeed, some attempts to use stochastic resonance in data transmission field have been recently reported [25–27]. However, neither the models used in these recent studies nor those found in the stochastic resonance literature in general, can be evidently deemed relevant to this field. As a matter of fact, being almost of reaction-diffusion type (i.e., overdamped systems) [14–16,19,28–30], these systems do not support such solitons as those derived from the nonlinear Schrödinger equation which is yet the framework of nonlinear optical telecommunications [31]. It therefore seems more appropriate to investigate model supporting nonlinear Schrödinger (NLS) soliton rather than model of reaction diffusion type to reliably establish stochastic resonance effect on data transmission field; which is the main aim of this article.

For this purpose, we consider a nonlinear discrete transmission line with a pass-band dispersion relation, excited at its left end by a sinusoidal driving whose frequency and amplitude do not allow any information transmission. We investigate how an additive noise can induce the generation of a soliton in the nonlinear medium and thus allow the transmission of the sinusoidal excitation.

The paper is organized as follows. In Sec. II, our model is presented. The description of the numerical procedure and the obtained results are developed in Sec. III. Moreover, using the probability of generating a soliton, the power spectrum and the SNR along the lattice, we also detail how noise enhances the transmission of the sinusoidal driving. Finally, Sec. IV is devoted to our conclusion.

II. MODEL

The system under consideration is one that has been studied extensively, both theoretically and experimentally by sev-

*Permanent address: Laboratoire de Mécanique, Département de Physique, Faculté des Sciences, Université de Yaoundé I, B.P. 812 Yaoundé, Cameroon. Electronic address: Serge-Bruno.Yamgoue@u-bourgogne.fr; syamgoue@uycdc.uninet.cm
†Electronic address: smorfu@bourgogne.fr
‡Electronic address: marquie@u-bourgogne.fr

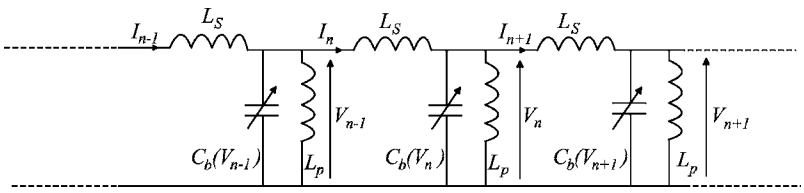

FIG. 1. Schematic representation of the electrical line.

eral authors [32–34]. It is modeled by the electrical nonlinear lattice of Fig. 1, in which L_s and L_p are linear inductors while C_b is a nonlinear capacitor. Applying Kirchhoff's laws to the array's elements at sites $n-1$, n, and $n+1$; and assuming that the capacitor-voltage characteristic of the nonlinear capacitor C_b is

$$C_b(V_n) = C_0(1 - 2\alpha V_n + 3\beta V_n^2), \tag{1}$$

one can establish that the voltage V_n is governed by the following equation

$$\frac{d^2V_n}{dt^2} + \omega_0^2 V_n + u_0^2(2V_n - V_{n+1} - V_{n-1}) = \frac{d^2}{dt^2}(\alpha V_n^2 - \beta V_n^3); \quad n = 1, \ldots, N. \tag{2}$$

This equation, in which we have set $w_0=(L_pC_0)^{-1/2}$ and $u_0=(L_sC_0)^{-1/2}$, models a nonlinear dispersive transmission line. It is well known that in such media the dispersion (due to the discreteness effects and to the natural gap induced by ω_0) can be balanced by the nonlinearity to give rise to a pulse-like wave called soliton; which propagates with constant velocity and profile [35]. Indeed, without the onsite nonlinearity, that is in the linear case, the pulse would spread out and disperse as it propagates.

The array is driven at its left end by

$$V_0(t) = A\cos(\omega t) + \eta_0(t), \tag{3}$$

which corresponds to a sinusoidal signal of amplitude A and pulsation ω corrupted by an additive white noise $\eta_0(t)$. In this study, the noise is assumed to have a gaussian distribution and is characterized by its root mean square (RMS) amplitude σ. Moreover, the numerical values used in this paper for the linear capacitor, inductors and the nonlinear coefficients α and β are the same as in [32–34], that is: $C_0=320.0pF$, $L_s=220.0\mu H$, $L_p=470.0\mu H$, $\alpha=0.21V^{-1}$, and $\beta=0.0197V^{-2}$.

In the noiseless case ($\eta_0(t)\equiv 0$) and for weak amplitude driving A, the harmonic waves propagating in the network of Fig. 1 present an angular frequency ω and a wave number k obeying to the following dispersion relation

$$\omega^2 = \omega_0^2 + 4u_0^2 \sin^2\left(\frac{k}{2}\right). \tag{4}$$

This dispersion relation is depicted in Fig. 2 and corresponds to a typical bandpass filter, with a gap $f_0=\omega_0/2\pi$ and a cutoff frequency $f_{max}=\omega_{max}/2\pi=(\omega_0^2+4u_0^2)^{1/2}/2\pi$ due to the lattice effects. The numerical values of these frequencies are $f_0=410.39$ kHz and $f_{max}=1267.93$ kHz.

III. NUMERICAL PROCEDURE AND RESULTS

This section is devoted to the numerical investigation of noise effect on the behavior of the network for sinusoidal driving with frequencies exceeding f_{max}. The specific case $f=\omega/2\pi=1.01f_{max}$ is thoroughly studied when the two control parameters A and σ are varied.

A. Numerical procedure

Our numerical simulations are conducted for an array of $N=1175$ oscillators. We use the standard fourth order Runge-Kutta algorithm [36], with time step $dt=T/512$, where $T=2\pi/\omega$ is the period of the sinusoidal input signal. The Gaussian noise is generated by using a pseudorandom number generator in combination with the Box-Muller algorithm [37]. To diminish the effects of waves reflection in the system, we consider the so-called absorbing boundary at the free end of the array as in Ref. [38]. This is simulated by adding a viscous damping term $\gamma(n)\dot{V}_n$ to Eq. (2); with

$$\gamma(n) = \begin{cases} 0, & 1 \leqslant n \leqslant m; \\ a\left[1 + \tanh\left(\dfrac{2n - m - N}{2b}\right)\right], & n > m. \end{cases} \tag{5}$$

The parameters m, a, and b are chosen such that the damping coefficient $\gamma(n)$ varies progressively from zero to 2 on the last 10% oscillators of the array. Also, the signal is smoothly feeded into the array by considering

$$V_0(t) = (1 - e^{-t/\tau})(A\cos(\omega t) + \eta_0(t)) \tag{6}$$

instead of Eq. (3); τ being some positive constant that we took equal to $30T$.

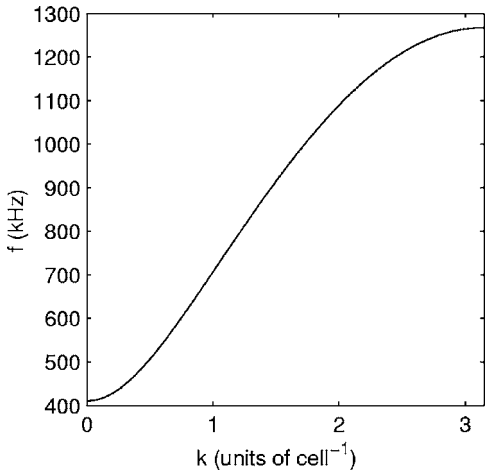

FIG. 2. Graph of the dispersion relation.

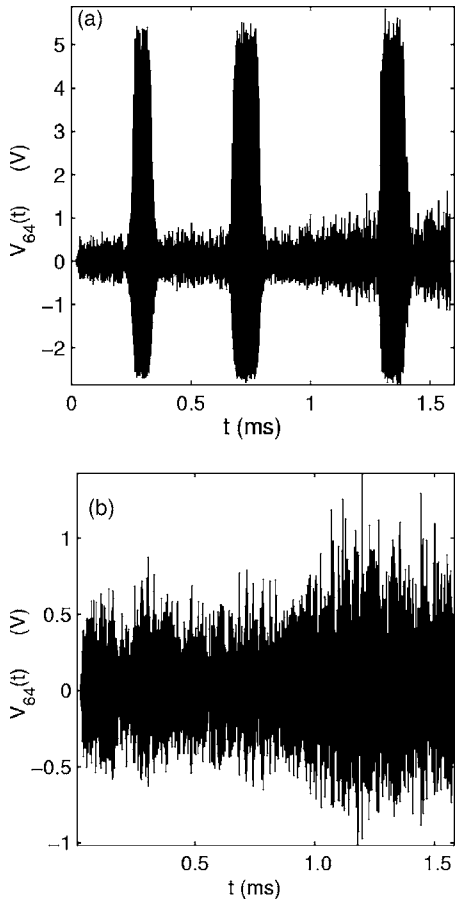

FIG. 3. Typical time series of (a) solitonic and (b) nonsolitonic structures evolving in the array (cell 64 here). Parameter values are $f=1.01f_{max}$, $A=1.9V$, and $\sigma=5V_{RMS}$.

We perform up to 150 runs for each value of the noise intensity σ, starting the array always from rest, i.e., with initial conditions

$$V_n(0) = \dot{V}_n(0) = 0; \quad n = 1, \ldots, N. \tag{7}$$

The integration time for each run is defined as $T_{max} = N/v_g(\omega)$, where

$$v_g(\omega) = \frac{1}{2\omega}\sqrt{|(\omega^2 - \omega_0^2)(\omega^2 - \omega_{max}^2)|} \tag{8}$$

is the formal expression of the linear group velocity. We deem this integration time long enough for our purpose since it covers up to 2780 periods of the driving for the frequency value considered herein. During this integration, the time evolution $V_n(t)$ for a few dozen of selected n are recorded at evenly spaced intervals in time. Our sampling time Δt is computed in a way to get a total of 16384 data covering the whole integration time defined above. Then, as in [19,28], the Fourier components of the spectrum of this time series at the first two harmonics of the forcing frequency:

$$P_n^{(k)} = (P_{sin}^{(k)})^2 + (P_{cos}^{(k)})^2, \quad k = 1,2, \tag{9}$$

with

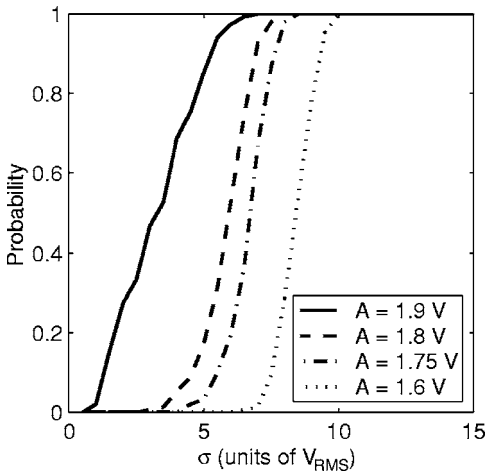

FIG. 4. Dependence of the probability of generating soliton on the gaussian noise RMS amplitude σ for various values of the signal amplitude and for $f=1.01f_{max}$.

$$P_{sin}^{(k)} = \frac{1}{T}\int_0^T V_n(t)\sin(k\omega t)dt, \quad P_{cos}^{(k)} = \frac{1}{T}\int_0^T V_n(t)\cos(k\omega t)dt \tag{10}$$

are computed by standard FFT algorithm [37] and used together with the usual signal-to-noise ratio

$$R_{SN} = 10\log_{10}\left(\frac{P_n^{(1)}}{p_n^{(1)}}\right) \tag{11}$$

to characterize the response of our medium in presence of noise. Here $p_n^{(1)}$ is the background noise power at the input signal's frequency and was estimated by simple linear interpolation [28].

B. Results

We begin by providing in Fig. 3 the time series of the typical structures obtained from the numerical integration of Eq. (2). Solitonic and nonsolitonic structures [Fig. 3(a) and Fig. 3(b), respectively] can clearly be distinguished in the noisy case. Since the frequency of the input signal lies in the linear gap of the system, one might wonder whether the generation of such a solitonic structure is a pure noise effect. We recall that our model is known to sustain the propagation of various types of soliton, including holes and pulses, when the frequency of the input signal belongs to the allowed band of the system. Their existence can be established as the solution of a NLS equation derived from Eq. (2) by using the reductive perturbation method [32–34]. This fact and the ubiquitous nature of the NLS equation in nonlinear physics, and more specifically to the description of optical telecommunications [31,39], have motivated our interest to the present model and provide strong conjecture on the importance of our investigation. For the case actually considered where the input signal's frequency belongs to the forbidden gap, recent studies on discrete deterministic systems driven at one end by a *periodic* signal have revealed that solitons can be generated if the signal's amplitude exceeds some critical value

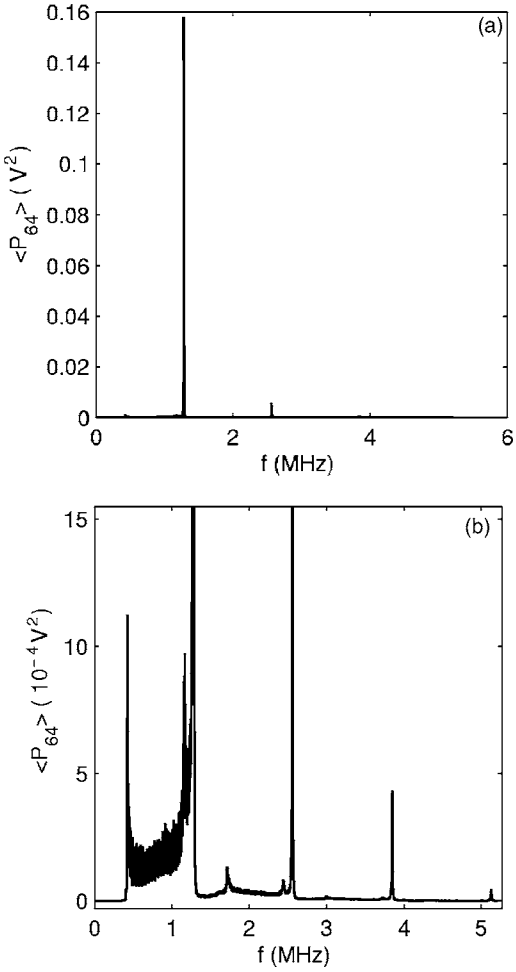

FIG. 5. Averaged PSD for solitonic structures at different scales. Parameter values are $f=1.01f_{max}$, $A=1.9V$, and $\sigma=9V_{RMS}$.

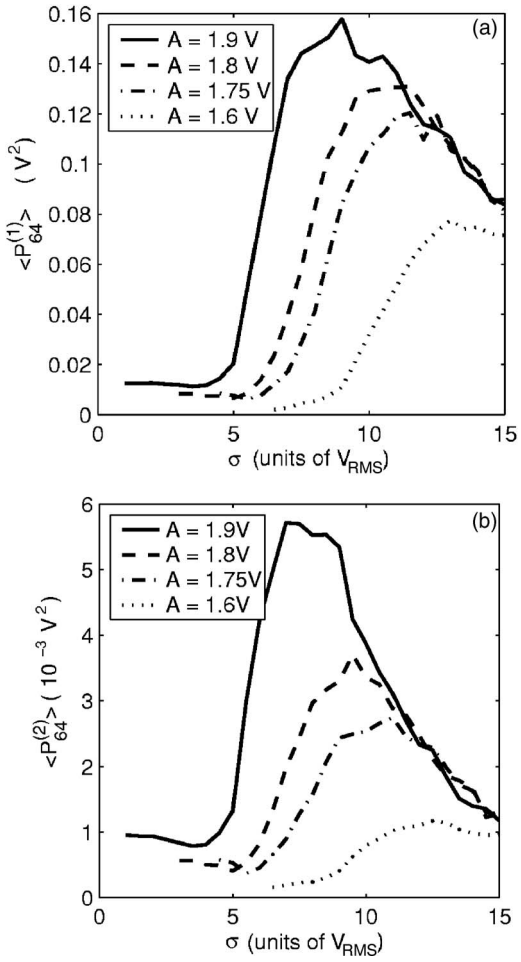

FIG. 6. Variation of the averaged PSD at cell $n=64$ as a function of the gaussian noise RMS amplitude σ for various values of the signal amplitude and for $f=1.01f_{max}$. (a): PSD at frequency f; (b): PSD at frequency $2f$.

[38,40,41]. Until now, both Sine Gordon and Klein Gordon chains as well as Fermi-Pasta-Ulam chains have revealed the possibility to exhibit this so-called "supratransmission" phenomenon. So, we have performed a preliminary numerical investigation to determine this threshold of "supratransmission" in the specific case of our nonlinear discrete transmission line. For the frequency value $f=1.01f_{max}$ considered herein, we have then observed that no supratransmission occurs for $A<1.9263V=A_{th}$. Therefore noise essentially fosters the occurrence of supratransmission in a parameter range where it can otherwise not be observed. Note that the noise effects on this so-called "supratransmission" is also without doubt of interest for its expected engineering applications [39,42].

The influence of noise on the propagation of these distinct structures necessarily needs to be distinguished. For this purpose, the 150 realizations considered for each noise intensity σ were divided into two parts: one consisting of realizations that generate solitonic structures and the other for those that do not. The results presented in this article are obtained by averaging the quantity defined in Eq. (9) over each part. Based on the results of the analysis of sample structures like that of Fig. 3(a) for different noise intensities, we define solitonic structure by the condition that

$$\max(V_{64}(t)) \geqslant 4.5V. \tag{12}$$

The choice of cell 64 in this definition is arbitrary; any other cell sufficiently far from the input end to reveal almost only noise effects, but also sufficiently close to that end to not miss any of these features could well be used.

With these setup at hand, the first interesting measure to quantify the effect of noise in our system is the probability of generating solitonic structures which is represented in Fig. 4. Note that, the probability of generating nonsolitonic structures is obviously the complement of that of solitonic structures, i.e., it is obtained by subtracting from unity. We can notice that the probability first remains almost constant to zero as σ is increased from zero up to some critical value, indicating that no or very few solitons are generated. Between this first critical value and a second one above which solitons are guaranteed to be generated for each realization, the increase of the noise intensity induces a rapid increase of the number of generated solitonic structures. This gives the probability curves the general profile of a staircase. Decreasing the signal's amplitude has the effect of shifting the critical values just mentioned to higher values.

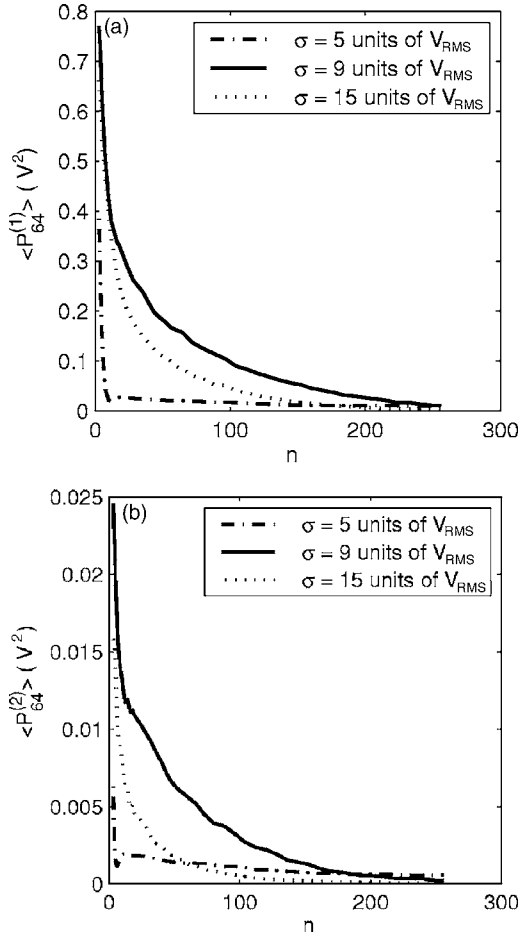

FIG. 7. Variation of the averaged PSD along the array for several values of the gaussian noise RMS amplitude σ, for $A=1.9V$, and $f=1.01f_{max}$. (a): PSD at frequency f; (b): PSD at frequency $2f$.

We now focus our attention on the influence of noise on the propagation process. We have deduced from Fig. 4 that nonsolitonic structures are dominantly generated for relatively weak noise intensities. However, our simulation results

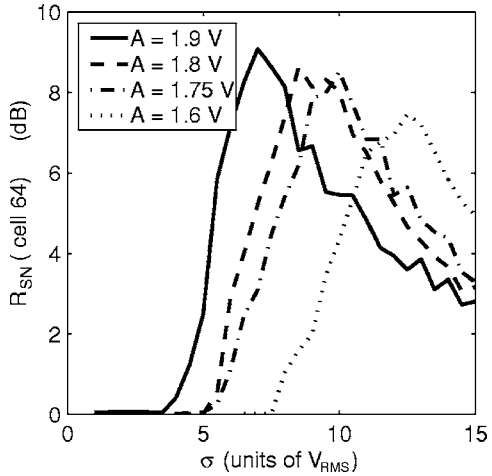

FIG. 8. Variation of the SNR at cell 64 ($R_{SN}(cell64)$) as a function of noise RMS amplitude for different signal amplitudes with $f=1.01f_{max}$.

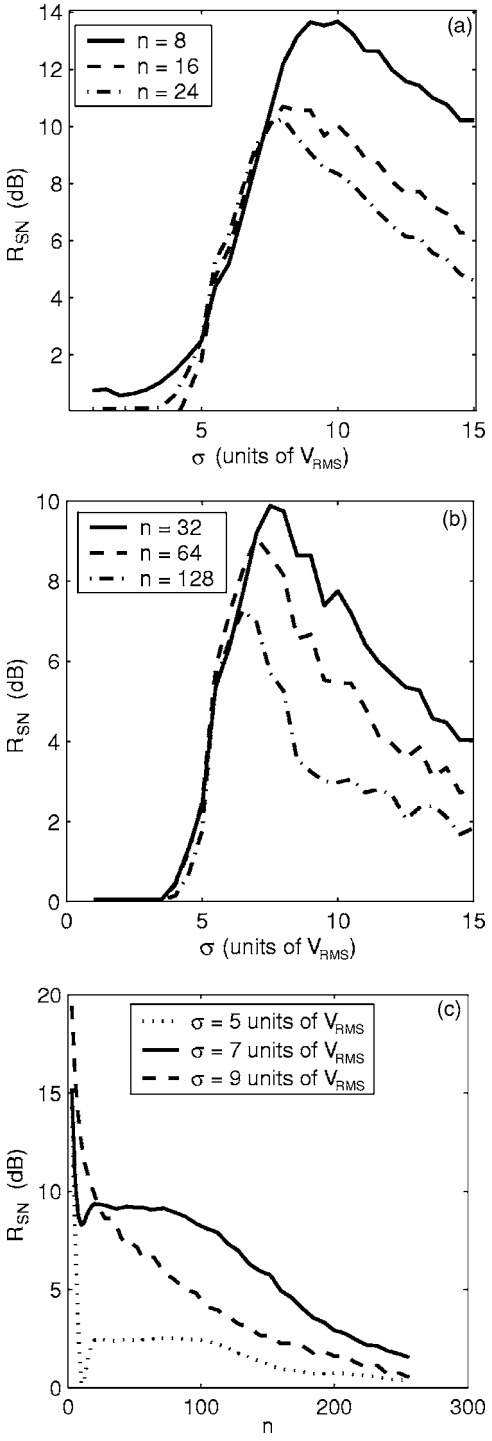

FIG. 9. Variation of the SNR (R_{SN}) as a function of noise RMS amplitude at various cells [(a) and (b)] and along the array (c) for various noise RMS amplitude when $A=1.9V$.

(not presented here) have shown that no appreciable improvement of nonsolitonic structure can be obtained for this range of noise intensity. In other words, the input signal is completely attenuated as in the deterministic case. Therefore we concentrate below on solitonic structures which, in fact, are the most interesting. An example of averaged power spectral density (PSD) for these structures is given in Fig. 5(a) and 5(b) in two different scales. We see from the first

scale that at most only the first two harmonics of the signal need be considered; while the second scale is necessary to reveal the background noise.

We depict in Fig. 6 the variation of the PSD as a function of the noise intensity for the cell 64. Both the first and second components of the PSD exhibit the classic stochastic resonance signature. The PSD increases with the increase of the noise up to a maximum which, for $A=1.9V$ for example, is attained for $\sigma_{opt}=9V_{RMS}$. Further increase of the noise level introduces disorder in the system and thus leads to the decrease of the PSD. We can also notice that a weaker maximum which is drifted to higher noises amplitudes is reached when the signal amplitude A is lowered.

To show that this observation is not specific to the cell 64, we plot in Fig. 7 the variation of the PSD as a function of n for σ_{opt} and two other values taken on both sides of it. We observe indeed that the relative order of the PSD corresponding to different noise intensities is preserved down the array, except very close to the input end. The optimum noise intensity in particular remains the same in the whole network.

The quantifier that we have considered at last in the evaluation of noise influence on the propagation is the well-known signal-to-noise ratio. Figures 8 and 9 summarize its behavior with respect to noise intensity as well as to the position in the array. All the features observed from the analysis of the PSD, including the existence of maxima with respect to σ [Fig. 8 and Fig. 9(a) and 9(b)], the effect of decreasing the signal's amplitude on these maxima [Fig. 8 and Fig. 9(a) and 9(b)] and the fact that the relative order of the SNRs corresponding to different noise intensities is preserved down the array [Fig. 9(c)], are confirmed. Notice however that the maxima for the SNR and the PSD are not attained for the same value of σ. In general the SNRs reach their maxima at smaller values of the noise intensity than the PSD ($\sigma'_{opt}=7V_{RMS}$ for $A=1.9V$). This is the simple traduction of the known fact that maximizing the output PSD with input noise do not guarantee maximal quality of the output signal, since the output noise might also increase with the input noise. It is particulary interesting to point out here the variation of the SNR for noise intensities less than or equal to the optimal one, with the specific characteristic of being quasi-constant for, say, the middle oscillators in the chain [$\sigma=5V_{RMS}$ and $\sigma=7V_{RMS}$ in Fig. 9(c)]. In contrast to the initial decrease of the SNR for the first few oscillators near the input which has been reported for arrays of overdamped oscillators [15], such constancy is related to the solitonic nature of the structures that are being propagating in the array. The cell number at which the SNR is minimum seems to be independent of the noise intensity: it might then correspond to the position at which the input signal would have completely died out in the absence of noise. From that point, the efficiency of noise shows up and thus the SNR increases. Finally, the later decrease of the SNR for oscillators sufficiently far from the input end can be explained by the fact that they were not reached by the solitons within our integration time.

IV. CONCLUSION

In this paper, we have numerically investigated the influence of noise on the transmission of a sinusoidal driving exciting a nonlinear discrete electrical line. We have focused specifically our study on the case where the input signal's frequency belongs to the natural gap of the line, so that without noise the nonlinear medium do not allow the transmission of the input signal.

We have shown that the information transmission is then possible adding an appropriate amount of gaussian noise. Indeed, our investigation reveals that the stochastic resonance phenomenon well studied for (array of) bistable, threshold and neural systems also occurs in a class of nonlinear waveguides. Especially, we have numerically established that noise can trigger the supratransmission phenomenon below its deterministic threshold with some probability. The variation of this probability with respect to the input noise amplitude is found to have a staircase profile. The propagation of the resulting solitons, measured by PSD and by SNR, presented remarkable resonant characteristics with respect to the amplitude of the applied noise. We noticed in particular the constancy of the SNR along the array for appropriate noise, which implies quality preserving signal transmission.

ACKNOWLEDGMENT

S.B.Y. acknowledges the financial support of the Conseil Régional de Bourgogne.

[1] R. Benzi, A. Sutera, and A. Vulpiani, J. Phys. A **14**, L453 (1981).
[2] R. Benzi, G. Parisi, A. Sutera, and A. Vulpiani, Tellus **34**, 10 (1982).
[3] C. Nicolis, Tellus **34**, 1 (1982).
[4] L. Gammaitoni, P. Hänggi, P. Jung, and F. Marcesoni, Rev. Mod. Phys. **70**, 223 (1998).
[5] N. G. Stocks, N. D. Stein, S. M. Soskin, and P. V. E. McClintock, J. Phys. A **25**, L1119 (1992).
[6] N. G. Stocks, N. D. Stein, and P. V. E. McClintock, J. Phys. A **26**, L385 (1993).
[7] M. Gitterman and G. H. Weiss, J. Stat. Phys. **70**, 107 (1993).
[8] J. F. Lindner, B. J. Breen, M. E. Wills, A. R. Bulsara, and W. L. Ditto, Phys. Rev. E **63**, 051107 (2001).
[9] A. Longtin, J. Stat. Phys. **70**, 309 (1993).
[10] A. Bulsara, E. W. Jacobs, T. Zhou, F. Moss, and L. Kiss, J. Theor. Biol. **152**, 531 (1991).
[11] F. Chapeau-Blondeau, X. Godivier, and N. Chambet, Phys. Rev. E **53**, 1273 (1996).
[12] F. Chapeau-Blondeau and X. Godivier, Phys. Rev. E **55**, 1478–1495 (1997).
[13] F. Chapeau-Blondeau, Phys. Rev. E **61**, 940–943 (2003).
[14] J. F. Lindner, B. K. Meadows, W. L. Ditto, M. E. Inchiosa, and A. R. Bulsara, Phys. Rev. Lett. **75**, 3 (1995).

[15] J. F. Lindner, S. Chandramouli, A. R. Bulsara, M. Löcher, and W. L. Ditto, Phys. Rev. Lett. **81**, 5048 (1998).
[16] R. Báscones, J. Garcia-Ojalvo, and J. M. Sancho, Phys. Rev. E **65**, 061108 (2002).
[17] S. Morfu, J. C. Comte, J. M. Bilbault, and P. Marquié, Int. J. Bifurcation Chaos Appl. Sci. Eng. **12**, 629 (2002).
[18] S. Morfu, Phys. Lett. A **317**, 73 (2003).
[19] A. Zaikin, D. Topaj, and J. García-Ojalvo, Fluct. Noise Lett. **2**, L47 (2002).
[20] E. Fermi, J. R. Pasta, and S. M. Ulam, *Studies of Nonlinear Problems*, in Collected Papers of E. Fermi, Vol. II (University of Chicago Press, Chicago, 1965), pp. 977–988.
[21] A. C. Scott, F. Y. F. Chu, and D. McLaughlin, Proc. IEEE **61**, 1443 (1973).
[22] E. Infeld and G. Rowland, *Nonlinear Waves, Solitons and Chaos* (Cambridge University Press, NY, 1990).
[23] V. E. Zakharov and S. Wabnitz, *Optical Solitons: Theoretical Challenges and Industrial Perspectives* (Springer-Verlag, Berlin, 1998).
[24] G. P. Agrawal, *Fiber-Optic Communication Systems*, 3rd ed. (Wiley Inter-Science, New York, 2002).
[25] S. Morfu, J. M. Bilbault, and J. C. Comte Int. J. Bifurcation Chaos Appl. Sci. Eng. **13**, 233 (2003).
[26] J. C. Comte and S. Morfu, Phys. Lett. A **305**, 39 (2003).
[27] F. Dua, D. Abott, and D. McLaughlin, Phys. Lett. A **344**, 401 (2005).
[28] Y. Zhang, G. Hu, and L. Gammaitoni, Phys. Rev. E **58**, 2952 (1998).
[29] N. Sungar, J. P. Sharpe, and S. Weber, Phys. Rev. E **62**, 1413 (2000).
[30] J. P. Sharpe, N. Sungar, M. Swaney, K. Carrigan, and S. Wheeler, Phys. Rev. E **67**, 056222 (2003).
[31] M. J. Ablowitz, B. Prinari, and A. D. Trubatch, *Discrete and Continuous Nonlinear Schrödinger Systems*, London Mathematical Society Lecture Note Series, 302 (2004).
[32] P. Marquié, J. M. Bilbault, and M. Remoissenet, Phys. Rev. E **49**, 828 (1994).
[33] J. M. Bilbault, P. Marquié, and B. Michaux, Phys. Rev. E **51**, 817 (1995).
[34] D. Yemélé, P. Marquié, and J. M. Bilbault, Phys. Rev. E **68**, 016605 (2003).
[35] M. Remoissenet, *Waves called Soliton: Concepts and Experiments*, 3rd ed. (Springer-Verlag, Berlin, 1999).
[36] M. Abramowitz and I. A. Stegun, *Handbook of Mathematical Functions with Formulas, Graphs, and Mathematical Tables*, 9th printing (Dover, New York, 1972).
[37] W. H. Press, B. P. Flannery, S. A. Teukolsky, and W. T. Vetterling, *Numerical Recipes in FORTRAN: The Art of Scientific Computing*, 2nd ed. (Cambridge University Press, Cambridge, U.K., 1992).
[38] F. Geniet and J. Leon, J. Phys.: Condens. Matter **15**, 2933 (2003).
[39] R. Khomeriki, Phys. Rev. Lett. **92**, 063905 (2004).
[40] F. Geniet and J. Leon, Phys. Rev. Lett. **89**, 134102 (2002).
[41] R. Khomeriki, S. Lepri, and S. Ruffo, Phys. Rev. E **70**, 066626 (2004).
[42] R. Khomeriki and J. Leon, Phys. Rev. E **71**, 056620 (2005).